

hep-ph/9909254
CERN-TH/99-252
FTUAM-99-25
FTUV/99-59
IFIC/99-62

Neutrino mixing and CP-violation

A. Donini^{a,1}, M.B. Gavela^{a,2}, P. Hernández^{b,3} and S. Rigolin^{a,4}

^a Dept. de Física Teórica, Univ. Autónoma de Madrid, 28049 Spain

^b Theory Division, CERN, 1211 Geneva 23, Switzerland

Abstract

The prospects of measuring the leptonic angles and CP-odd phases at a neutrino factory are discussed in two scenarios: 1) three active neutrinos as indicated by the present ensemble of atmospheric plus solar data; 2) three active plus one sterile neutrino when the LSND signal is also taken into account. For the latter we develop one and two mass dominance approximations. The appearance of wrong sign muons in long baseline experiments and tau leptons in short baseline ones provides the best tests of CP-violation in scenarios 1) and 2), respectively.

¹donini@daniel.ft.uam.es

²gavela@garuda.ft.uam.es

³pilar.hernandez@cern.ch. On leave from Dept. de Física Teórica, Universidad de Valencia.

⁴rigolin@daniel.ft.uam.es

1 Introduction

The putative value of the masses and mixing angles of the leptonic sector are part of the fundamental problem usually dubbed “flavour puzzle”. The comprehension of the origin of these parameters and the analogous ones in the quark sector, together with the overall understanding of the origin of masses attempted through Higgs searches, constitutes one of the most passionating research subjects today in particle physics. The precise determination of those parameters is a mandatory first step.

After many years of experimental quest, exciting neutrino data pointing towards neutrino oscillations, and thus neutrino masses and mixing angles, are starting to be available:

- The SuperKamiokande [1] data on atmospheric neutrinos are interpreted as oscillations of muon neutrinos into neutrinos that are not ν_e s. Roughly speaking, the measured mixing angle is close to maximal, $\sin^2 2\theta > 0.8$, and Δm^2 is in the range 2 to $6 \times 10^{-3} \text{ eV}^2$, all at 90% confidence level.
- The solar neutrino deficit is interpreted either as MSW (matter enhanced) oscillations [2] or as vacuum oscillations [3] that deplete the original ν_e s, presumably in favour of ν_μ s or alternatively into sterile neutrinos. The corresponding squared mass differences (10^{-5} to 10^{-4} eV^2 or some 10^{-10} eV^2) are significantly below the range deduced from atmospheric observations.
- The LSND signal [4] could indicate, if confirmed, ν_e s oscillating into ν_μ s (and $\bar{\nu}_e$ s into $\bar{\nu}_\mu$ s) with $\Delta m^2 \sim 0.3 - 1 \text{ eV}^2$ and $10^{-3} < \sin^2 2\theta < 1$ mixing angle.

The atmospheric plus solar data can be easily accommodated in a three family mixing scenario, with two distinct mass differences. LEP data restricts the number of active neutrino species to three. Thus, when the LSND signal is also taken into account, its associated new mass difference requires the consideration of a supplementary sterile neutrino [5]. In either case, the physical parameters present in the neutrino Yukawa sector can be parametrized “a la CKM”, as in the quark sector, with the addition of extra phases if the neutrinos are Majorana particles.

Oscillation experiments are sensitive to mass differences, mixing angles and Dirac phases, and not to Majorana phases. After further confirmation of the present data, a future experimental neutrino program should aim at the precise determination of these parameters. A *neutrino factory* from muon storage rings [6] would provide very intense, pure and flavour-rich neutrino beams, well suited for precision studies and even the discovery of leptonic CP violation, since the two polarities of the beam are available. From a μ^- beam, the following transitions can be explored:

$$\begin{aligned} \mu^- &\rightarrow e^- \quad \nu_\mu \quad \bar{\nu}_e; \\ \bar{\nu}_e &\rightarrow \bar{\nu}_e \rightarrow e^+ \text{ disappearance,} \end{aligned}$$

$$\begin{aligned}
& \bar{\nu}_e \rightarrow \bar{\nu}_\mu \rightarrow \mu^+ \text{ appearance,} \\
& \bar{\nu}_e \rightarrow \bar{\nu}_\tau \rightarrow \tau^+ \text{ appearance } (\tau^+ \rightarrow \mu^+; e^+), \\
& \nu_\mu \rightarrow \nu_\mu \rightarrow \mu^- \text{ disappearance,} \\
& \nu_\mu \rightarrow \nu_e \rightarrow e^- \text{ appearance,} \\
& \nu_\mu \rightarrow \nu_\tau \rightarrow \tau^- \text{ appearance } (\tau^- \rightarrow \mu^-; e^-). \tag{1}
\end{aligned}$$

The “wrong sign” channels of μ^+ , τ^+ and e^- appearance, for which there would be no beam-induced background at the neutrino factory, are the good news with respect to other type of neutrino beams.

In this work, we consider convenient parametrizations of the physical mixing angles and CP phases in the cases of three and four neutrino species, and study their experimental signals at the neutrino factory.

For the sake of illustration, we shall consider as a “reference set-up” the neutrino beams resulting from the decay of $n_\mu = 2 \times 10^{20} \mu^+$ s and/or μ^- s in a straight section of an $E_\mu = 10 - 50$ GeV muon accumulator ring. Muon energies of 40 – 50 GeV are at present under discussion [8] as a convenient goal, as they allow good background rejection [9] and do not preclude the exploration of neutrino signals at lower energies. This is because the number of neutrinos in a given energy bin does not depend on the parent muon energy, while the total number of oscillated and interacted neutrinos increases with E_μ [6].

For just three active neutrino species, where the dominant signals peak at “atmospheric” distances, we consider a long baseline (LBL) experiment located some 732 km downstream, roughly the distance from CERN to Gran Sasso or from Fermilab to the Soudan Lab. For this scenario we first update the study of CP-odd observables performed in [7]. Higher intensity fluxes are also considered for CP-odd signals. We further discuss the scaling laws that relate the sensitivities at different energies and distances.

In the case of three active plus one sterile neutrino, most of the parameter space can be explored in experiments at short baseline distances (SBL) of $\mathcal{O}(1\text{-}10 \text{ km})$.

The paper is organized as follows. In section 2 we update the analysis of the three family scenario and derive the scaling laws for the CP-odd observables. Section 3 deals with the four species scenario. One and two mass scale dominance schemes are derived, and the sensitivity to angles and CP-odd phases, relevant in this scheme, are explored. We conclude in section 4.

2 Update of three-family analysis

Let us adopt, from solar and atmospheric experiments, the indication that $|\Delta m_{solar}^2| \ll |\Delta m_{atm}^2|$, dubbed “minimal” or “one mass scale dominance” scheme. Atmospheric or terrestrial experiments have an energy range such that $\Delta m^2 L / E_\nu \ll 1$ for the smaller

but not necessarily for the larger of these mass gaps. Even then, solar and atmospheric (or terrestrial) experiments are not two separate two-generation mixing effects in general. Given this hierarchy of mass differences and assigning $\Delta m_{solar}^2 = \Delta m_{12}^2$, $\Delta m_{atm}^2 = \Delta m_{23}^2$, it is convenient to use the standard 3-family mixing parametrization of the PDG,

$$U = U_{23}(\theta_{23})U_{13}(\theta_{13}, \delta)U_{12}(\theta_{12}), \quad (2)$$

for the mixing angles and phase. In the approximation $\Delta m_{12}^2 = 0$, one physical angle and one phase should become unphysical. This is cleanly achieved in this parametrization, where the rotation matrix, U_{12} , associated with the two degenerate eigenstates, is located to the right of eq. (2). In this way, the angle θ_{12} drops out of the neutrino mass matrix when the solar mass difference is neglected⁵ and the relevant parameters for the atmospheric oscillation are reduced to the smaller set $(\theta_{23}, \Delta m_{23}^2$ and $\theta_{13})$.

From now on we separate the CP-even terms from the CP-odd ones in the transition probabilities in the following way,

$$P(\nu_\alpha \rightarrow \nu_\beta) = P_{CP}(\nu_\alpha \rightarrow \nu_\beta) + P_{CP}(\nu_\alpha \rightarrow \nu_\beta). \quad (3)$$

For atmospheric distances, the CP-even components of the transition probabilities are accurately given by

$$\begin{aligned} P_{CP}(\nu_e \rightarrow \nu_\mu) &= \sin^2(\theta_{23}) \sin^2(2\theta_{13}) \sin^2\left(\frac{\Delta m_{23}^2 L}{4E_\nu}\right) \\ P_{CP}(\nu_e \rightarrow \nu_\tau) &= \cos^2(\theta_{23}) \sin^2(2\theta_{13}) \sin^2\left(\frac{\Delta m_{23}^2 L}{4E_\nu}\right) \\ P_{CP}(\nu_\mu \rightarrow \nu_\tau) &= \cos^4(\theta_{13}) \sin^2(2\theta_{23}) \sin^2\left(\frac{\Delta m_{23}^2 L}{4E_\nu}\right), \end{aligned} \quad (4)$$

provided the solar mass difference is much smaller than the atmospheric one. Generically all flavour transitions occur with the same sinusoidal dependence on $\Delta m_{23}^2 L/E_\nu$. Notice that for $\theta_{13} = 0$ the probability $P(\nu_\mu \rightarrow \nu_\tau)$ reduces to the two-family (2-3) mixing expression, while the other probabilities vanish.

An analysis of the sensitivity of the neutrino factory to the transitions above was already done in [7]. After that work, detailed background estimations have been performed [9]. The overall conclusion is that the neutrino factory can reach much higher precision in the determination of the parameters involved in the atmospheric oscillation than any other planned facility. For instance, while all other planned experiments will reach at most sensitivities of $\sin^2(\theta_{13}) > 10^{-2}$, much lower values are attainable at the neutrino factory, down to $\sin^2(\theta_{13}) > 10^{-4}$. This is important if the value of this angle turns out to be as small as suggested by present data, which set the best fit value at $\sin^2(\theta_{13}) = 2 \times 10^{-2}$ [10].

⁵Notice that this would not happen automatically for a different ordering in eq. (2)

2.1 CP violation

The CP-odd terms in eq. (3) vanish when $\Delta m_{12}^2 L/E_\nu$ effects are neglected, as they should, because the CP-phase of the mixing matrix can then be rotated away. The first non-trivial order gives, to leading order in the solar mass difference,

$$\begin{aligned} P_{\mathcal{CP}}(\nu_e \rightarrow \nu_\mu) &= P_{\mathcal{CP}}(\nu_\mu \rightarrow \nu_\tau) = -P_{\mathcal{CP}}(\nu_e \rightarrow \nu_\tau) \\ &= -8c_{12}c_{13}^2c_{23}s_{12}s_{13}s_{23} \sin \delta \left(\frac{\Delta m_{12}^2 L}{4E_\nu} \right) \sin^2 \left(\frac{\Delta m_{23}^2 L}{4E_\nu} \right). \end{aligned} \quad (5)$$

As found in [7], any hope of observability requires that nature chooses Δm_{12}^2 in the higher range allowed by solar experiments, $\Delta m_{12}^2 \sim 10^{-4} \text{eV}^2$, and that the “solar” mixing $\sin(2\theta_{12})$ is large. These values correspond to the large mixing angle solution (LMA-MSW) of the solar deficit. Other analyses of the observability of CP violation in the leptonic sector have been presented in [11] and [12]. Previous theoretical work can be found also in [13].

We first summarize the results for the CP-odd asymmetry [14] obtained in [7], and update the analysis for different E_μ and higher intensities of the muon beam.

Consider the CP-asymmetry

$$A_{\alpha\beta}^{CP} \equiv \frac{P(\nu_\alpha \rightarrow \nu_\beta) - P(\bar{\nu}_\alpha \rightarrow \bar{\nu}_\beta)}{P(\nu_\alpha \rightarrow \nu_\beta) + P(\bar{\nu}_\alpha \rightarrow \bar{\nu}_\beta)}, \quad (6)$$

which, in vacuum, would be a CP-odd observable. Given the present experimental constraints, the largest asymmetry is expected in the $(e\mu)$ -channel. The voyage through our CP-uneven planet induces a non-zero $A_{e\mu}^{CP}$ even if CP is conserved, since ν_e and $\bar{\nu}_e$ are differently affected by the ambient electrons [13]. In a neutrino factory $A_{e\mu}^{CP}$ would be measured by first extracting $P(\nu_\mu \rightarrow \nu_e)$ from the produced (wrong-sign) μ^- s in a beam from μ^+ decay and $P(\bar{\nu}_e \rightarrow \bar{\nu}_\mu)$ from the charge conjugate beam and process. Notice that even if the fluxes are very well known, this requires a good knowledge of the cross section ratio $\sigma(\bar{\nu}_\mu \rightarrow \mu^+)/\sigma(\nu_\mu \rightarrow \mu^-)$, which may be gathered in a short baseline experiment. To obtain information on the genuinely CP-odd phase, the matter effects in the oscillation probabilities must also be known with sufficient precision.

A central question on the observability of CP-violation is that of statistics. In practice, for our reference set-up, there would be too few events to exploit the explicit E_ν dependence of the CP-odd effect. To construct a realistic CP-odd observable consider the neutrino-energy integrated quantity:

$$\bar{A}_{e\mu}^{CP}(\delta) = \frac{\{N[\mu^-]/N_o[e^-]\}_+ - \{N[\mu^+]/N_o[e^+]\}_-}{\{N[\mu^-]/N_o[e^-]\}_+ + \{N[\mu^+]/N_o[e^+]\}_-}, \quad (7)$$

where the sign of the decaying muons is indicated by a subindex, $N[\mu^+]$ ($N[\mu^-]$) are the measured number of wrong-sign muons, and $N_o[e^+]$ ($N_o[e^-]$) are the expected number of $\bar{\nu}_e$ (ν_e) charged current interactions in the absence of oscillations. In order to quantify

the significance of the signal, we compare the value of the integrated asymmetry with its error, in which we include the statistical error and a conservative background estimate at the level of 10^{-5} .

The measurement of $\bar{A}_{e\mu}^{CP}(\delta)$ at the neutrino factory was considered in [7] with matter effects taken into account. It was concluded that, for 2×10^{20} useful muons, if the neutrino mass differences are those indicated by the ensemble of solar and atmospheric observations and the physics is that of three standard families, there was little hope to observe CP-violation with the beams and detectors under discussion. Nevertheless, it has been recently pointed out [8] that it is technically feasible to rise the muon flux intensity by about one order of magnitude with respect to our “reference set-up”. If the solar LMA solution is confirmed in the coming years, such upgrading may allow to unravel CP-violation in the neutrino sector, would the CP-odd phase, δ , be sizable.

The asymmetry in eq. (7) does not vanish when the CP-phase does due to matter effects. In order to illustrate the true sensitivity to the CP-odd phase, we consider the subtracted asymmetry $|\bar{A}_{e\mu}^{CP}(\pi/2) - \bar{A}_{e\mu}^{CP}(0)|$, i.e. the difference between the asymmetry at the maximum value of the CP-phase, $\delta = \pi/2$, and that at $\delta = 0$. Of course, if the subtracted term is large, performing this theoretical subtraction in practice would require a very precise knowledge of matter effects and also of the remaining oscillation parameters. Fig. 1 displays the signal-over-noise ratio for the subtracted asymmetry as a function of distance, for 2×10^{20} (left) and 2×10^{21} (right) useful muons and for a 10 kTon detector. The oscillation parameters in Fig. 1 are chosen to be: $\Delta m_{12}^2 = 10^{-4}$ eV², $\Delta m_{23}^2 = 2.8 \times 10^{-3}$ eV², $\theta_{12} = 22.5^\circ$, $\theta_{13} = 13^\circ$ and $\theta_{23} = 45^\circ$ with the phase $\delta = -\pi/2$ in the convention of the PDG. The value chosen for Δm_{23}^2 is the central one of the most recent SuperKamiokande analysis [1] [10]: 2.8×10^{-3} eV². When obtaining this figure (as well as in the following ones concerning CP-violation) the exact theoretical expressions have been used.

For 2×10^{21} useful muons, the number of “standard deviations” is seen to exceed a comfortable ~ 5 at a large range of distances, with a peak towards 3000 km.

Let us discuss the relative size of the matter induced asymmetry versus the true CP signal (i.e. the terms in the asymmetry proportional to $\sin \delta$). For $\theta_{13} = 13^\circ$ (which is the present upper bound from Chooz [15]) and at moderate energies, $E_\mu = 10, 20$ GeV, its contribution is 3 – 4 times larger than the true CP-signal, which is around 5% – 10%, and thus it is necessary to know the subtracted term with a precision better than 20% in order to extract any information on δ . At higher energy, $E_\mu = 50$ GeV, the situation gets worse: the matter induced asymmetry turns out to be much larger than the true CP-signal, which is of the order of a few per cent. It does not seem realistic to expect to know the error in the (by then hypothetically measured) leptonic parameters with sufficient precision to measure the true CP signal in this case. On the other hand, analyzing the energy dependence of the signal may be feasible at the larger statistics available at this high energy, which might allow a cleaner separation of matter effects from CP violating ones. This possibility will be studied in the future.

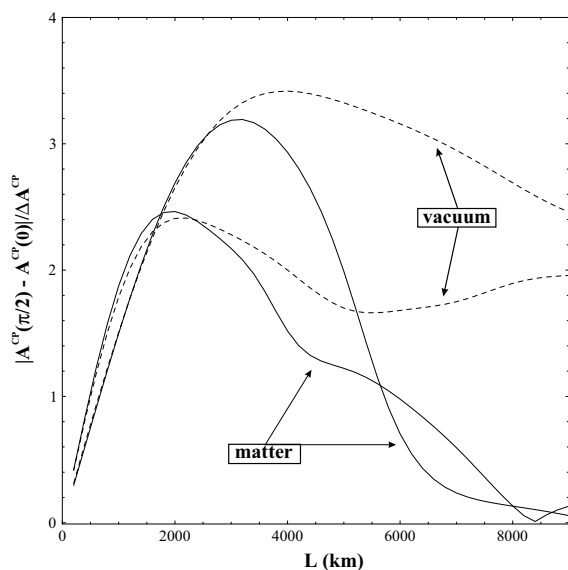


Figure 1: *Signal over statistical uncertainty for $|\bar{A}_{e\mu}^{CP}(\pi/2) - \bar{A}_{e\mu}^{CP}(0)|$ as a function of distance. Continuous (dashed) lines correspond to matter (vacuum) oscillations. In the left side, lower and upper curves correspond to $E_\mu = 10, 20$ GeV for 2×10^{20} useful muons/year. In the right the same is depicted for $E_\mu = 20, 50$ GeV and 2×10^{21} useful muons/year. The chosen CKM parameters are as described in the text.*

It is important to realize, however, that the relative size of the true CP signal and the total asymmetry depends very much on the value of the angle θ_{13} in vacuum⁶. As θ_{13} is decreased, not only the term proportional to $\sin \delta$ in the asymmetry increases⁷ [11], but also the matter induced asymmetry decreases. As an example, for $E_\mu = 20$ GeV and $\theta_{13} = 5^\circ$, the matter induced asymmetry is of the same order as the true CP-signal and becomes five times smaller at $\theta_{13} = 1^\circ$. At this value, the true CP asymmetry becomes as large as 50%. The subtraction of the small matter induced asymmetry in this situation should be very easy. One should keep in mind, that although the present best fit value for θ_{13} is 8° , a much smaller value would also be in perfect agreement with atmospheric and solar data.

Up to here we have considered the experimental constraints resulting from the ensemble of the solar data. The CP-violation effects are much bigger for the larger mass differences that become possible if the results of some solar neutrino experiment are disregarded. This is because the CP asymmetry grows linearly with the solar mass difference. As an example, increasing Δm_{12}^2 from 10^{-4} eV² to 8×10^{-4} eV², with the other parameters fixed as in the left plot of Fig. 1, results in a very promising signal

⁶A more detailed discussion of the dependence on θ_{13} and matter effects will be presented elsewhere [16].

⁷Notice however, that the ratio of the asymmetry to its statistical error does not change, so 2×10^{21} useful muons would still be needed.

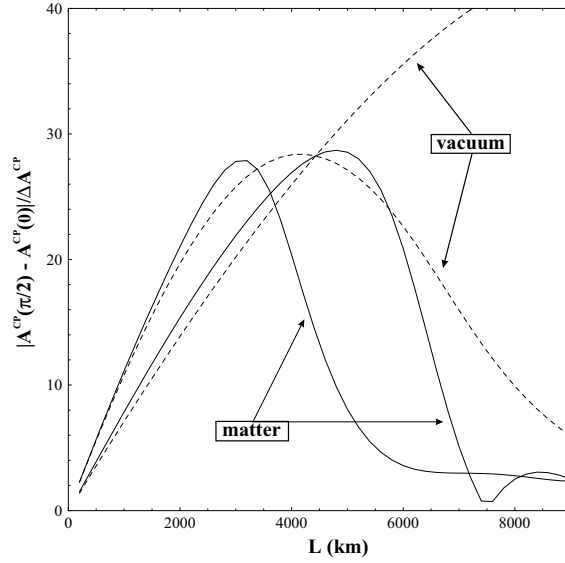


Figure 2: *Signal over statistical uncertainty for $|\bar{A}_{e\mu}^{CP}(\pi/2) - \bar{A}_{e\mu}^{CP}(0)|$ as a function of distance, for $\Delta m_{12}^2 = 8 \times 10^{-4} \text{ eV}^2$ and the rest of the parameters as in the left plot of Fig. 1.*

over noise ratio even in the “conservative” option of 2×10^{20} useful muons. This is depicted in Fig. 2.

In ref. [7] the T-odd asymmetry at the neutrino factory was as well briefly discussed. As it requires the measurement of the electron charge, which seems experimentally out of reach at present, we refrain from its further study in this paper.

2.2 Matter effects and scaling laws for CP-observables

It is interesting to understand how the sensitivities to mixing angles and CP-odd effects scale with LBL distances and beam energies. We concentrate here on CP-odd observables, since the CP-even ones were discussed in [7].

Consider the vacuum CP-odd observable defined in eq. (7). Neglecting the detection background and other systematic errors, the signal over its statistical error, depicted in Fig. 1, scales as

$$\frac{A_{e\mu}^{CP}}{\Delta A_{e\mu}^{CP}} = \frac{P_{CP} \sqrt{N_{CC}}}{\sqrt{P_{CP}}} \propto \sqrt{E_\nu} \left| \sin \left(\frac{\Delta m_{23}^2 L}{4E_\nu} \right) \right|, \quad (8)$$

where we have used that the number of charged currents scales as $N_{CC} \propto E_\nu^3/L^2$. Hence, the location of the maximum is at $\Delta m_{23}^2 L/E_\nu = 2\pi$ whereas the height scales with the square root of the energy.

	Height	Location
Vacuum	$\propto \sqrt{E_\nu}$	$L = \frac{2\pi E_\nu}{\Delta m_{23}^2}$
Matter	$\propto 1$	$L = \frac{\pi}{A}$

Table 1: *Height and location of the maximum of the CP-violating signal-to-noise ratio as a function of the neutrino energy E_ν and of the source-to-detector distance L in vacuum, and in matter for $A \gg \Delta m_{ij}^2$.*

In matter, the situation is somewhat more involved. First, the splitting between mass eigenstates in vacuum must be replaced by the splitting of the mass eigenstates in matter, thus affecting the location of the maximum in the signal-to-noise ratio. The second and most important difference is that the effective mixing angles in matter depend on the energy, thus modifying the scaling with the energy of the maximum height. In the regime in which the matter-induced mass splitting, $A = 2E_\nu\sqrt{2}G_F n_e$ (where n_e is the number density of electrons in the earth) is larger than all mass differences (Δm_{12}^2 and Δm_{23}^2) it is easy to show that only the effective angle θ_{13} changes significantly with the energy. More specifically, for the signal-to-noise ratio the angular difference between vacuum and matter relies on the effective $\cos(\theta_{13})$, which has a $1/\sqrt{E_\nu}$ functional dependence on energy. This factor cancels the $\sqrt{E_\nu}$ dependence of the signal-to-noise ratio in vacuum, and the height of the maximum does no longer scale with the energy. This behaviour can be seen in Fig. 1 where the signal-to-noise ratio is plotted both in vacuum and in matter at different values of the energy of the muon beam.

Table 1 summarizes the scaling laws of height and location of the CP-violating signal-to-noise ratio maximum as a function of E_ν and L , both in vacuum and in matter.

3 Four-Neutrino species

The LSND signal of $\nu_\mu \rightarrow \nu_e$ oscillations would indicate a third distinct neutrino mass range, $\Delta m_{LSND}^2 = 0.3 - 1 \text{ eV}^2$. It is then necessary to introduce a fourth light neutrino, a sterile one, in order to comply with the bounds on the number of neutrinos coupled to the Z^0 [18].

A combined analysis of the results for solar, atmospheric and LSND experiments points [19] towards a four neutrino pattern in which there are two nearly degenerate

Class I

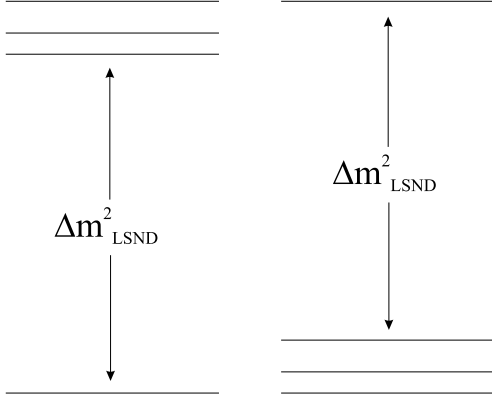


Figure 3: *Different type of four-neutrino families scenarios: Class-I scenarios (left); Class-II scenarios (right).*

neutrino pairs separated by a large mass gap, Δm_{LSND}^2 . Different scenarios are depicted in Fig. 3. Our analysis sticks to class-II, since class-I seems to be excluded by data [21].

Whatever the mechanism responsible for the neutrino masses, given n light neutrino species, oscillation experiments are only sensitive to a unitary $n \times n$ mixing matrix “a la CKM”: the effects of Majorana phases being suppressed by factors of m_ν/E_ν . In all generality, the parameter space of a four-species scenario would consist of six rotation angles and three complex phases if the neutrinos are Dirac fermions, while it spans six angles plus six phases if the neutrinos are Majorana fermions. Among the latter, three are pure Majorana phases and thus to be disregarded in what follows, reducing the analysis to the mentioned 4×4 “Dirac-type” system.

We assign the mass eigenstates in the following way:

$$\Delta m_{\text{sol}}^2 = \Delta m_{12}^2 \ll \Delta m_{\text{atm}}^2 = \Delta m_{34}^2 \ll \Delta m_{\text{LSND}}^2 = \Delta m_{23}^2. \quad (9)$$

Given the large hierarchy indicated by data, two approximations are useful:

1. $\Delta m_{12}^2 = \Delta m_{34}^2 = 0$, “one mass scale dominance” (or minimal) scheme,
2. $\Delta m_{12}^2 = 0$, “two mass scale dominance” (or next-to-minimal) scheme.

The number of independent angles and phases is then reduced as reported in Tab. 2. The minimal scheme is sufficient to illustrate the sensitivity to the mixing angles at the neutrino factory. In this approximation, a physical CP-odd phase is still present although not sufficient to produce CP-violation effects in neutrino oscillations. The next-to-minimal scheme is necessary to address the question of CP-violation, as two non-zero mass differences are required for producing observable effects, alike to the standard three-family scenario.

	Angles	Dirac CP-phases	Majorana CP-phases
Majorana ν 's	6	3	3
Dirac ν 's	6	3	0
Dirac ν 's $\Delta m_{12}^2 = 0$	5	2	0
Dirac ν 's $\Delta m_{12}^2 = \Delta m_{34}^2 = 0$	4	1	0

Table 2: *Parameter space for four neutrino families: for Dirac neutrinos we consider the general case with three non-zero mass differences and the particular case (considered in the rest of the paper) with one or two mass differences set to zero; for Majorana neutrinos we consider only the general case.*

A general rotation in a four dimensional space can be obtained by performing six different rotations U_{ij} in the (i, j) plane, resulting in plenty of different possible parametrizations of the mixing matrix, disregarding phases. We choose the following convenient parametrization, given the hierarchy of mass differences of eq. (9):

$$U = U_{14}(\theta_{14})U_{13}(\theta_{13})U_{24}(\theta_{24})U_{23}(\theta_{23}, \delta_3)U_{34}(\theta_{34}\delta_2)U_{12}(\theta_{12}, \delta_1). \quad (10)$$

As shown in Table 2, if a given mass difference vanishes the number of physical angles and phases gets reduced by one. A convenient parametrization of the angles is that in which the rotation matrices corresponding to the most degenerate pairs of eigenstates are placed to the extreme right. If the eigenstates i and j are degenerate and the matrix U_{ij} is located to the right in eq. (10), the angle θ_{ij} becomes automatically unphysical in this parametrization. If a different ordering is taken no angle disappears from the oscillation probabilities. A redefinition of the rest of the parameters would then be necessary in order to illustrate the remaining reduced parameter space in a transparent way. Our parametrization corresponds thus to the “cleanest” choice, having settled at the extreme right the rotations corresponding to the most degenerate pairs.

In the “one mass dominance” scheme, the pairs (θ_{12}, δ_1) and (θ_{34}, δ_2) decouple automatically. In the “two mass dominance” scheme, only the pair (θ_{12}, δ_1) does. Thus only the exact number of physical parameters, according to Table 2, remains both in the minimal and next-to-minimal schemes. Notice that it is also important to distribute the phases so that they decouple, together with the angles, when they should.

3.1 Sensitivity reach of the neutrino factory for four neutrino species

We concentrate now on the sensitivity to the different angles describing the system when only the big LSND mass difference is taken into account, that is the “one mass scale” approximation, discussed at the beginning of this section. Four rotation angles (θ_{13} , θ_{14} , θ_{23} and θ_{24}) and one complex phase (δ_3) remain. The two rotation angles that have become unphysical are already tested at solar (θ_{12} in our parametrization) and atmospheric (θ_{34}) neutrino experiments. The remaining four can be studied at the neutrino factory with high precision, due to the rich flavour content of the neutrino beam. Notice that the number of flavour transitions that can be measured is enough to constraint all these angles. We will concentrate for illustration on the following channels:

$$\begin{aligned}
\bar{\nu}_e &\rightarrow \bar{\nu}_\mu \rightarrow \mu^+ && (\mu^+ \text{appearance}) \\
\nu_\mu &\rightarrow \nu_\mu \rightarrow \mu^- && (\mu^- \text{disappearance}) \\
\bar{\nu}_e &\rightarrow \bar{\nu}_\tau \rightarrow \tau^+ && (\tau^+ \text{appearance}) \\
\nu_\mu &\rightarrow \nu_\tau \rightarrow \tau^- && (\tau^- \text{appearance}).
\end{aligned} \tag{11}$$

The corresponding probability transitions acquire a simple form:

$$P_{CP}(\nu_e \rightarrow \nu_\mu) = 4c_{13}^2 c_{24}^2 c_{23}^2 s_{23}^2 \sin^2 \left(\frac{\Delta m_{23}^2 L}{4E} \right), \tag{12}$$

$$P_{CP}(\nu_\mu \rightarrow \nu_\mu) = 1 - 4c_{13}^2 c_{23}^2 (s_{23}^2 + s_{13}^2 c_{23}^2) \sin^2 \left(\frac{\Delta m_{23}^2 L}{4E} \right), \tag{13}$$

$$\begin{aligned}
P_{CP}(\nu_e \rightarrow \nu_\tau) &= 4c_{23}^2 c_{24}^2 \left[(s_{13}^2 s_{14}^2 s_{23}^2 + c_{14}^2 c_{23}^2 s_{24}^2) \right. \\
&\quad \left. - 2c_{14} s_{14} c_{23} s_{23} s_{13} s_{24} \cos \delta_3 \right] \sin^2 \left(\frac{\Delta m_{23}^2 L}{4E} \right),
\end{aligned} \tag{14}$$

$$\begin{aligned}
P_{CP}(\nu_\mu \rightarrow \nu_\tau) &= 4c_{13}^2 c_{23}^2 \left[(s_{13}^2 s_{14}^2 c_{23}^2 + c_{14}^2 s_{23}^2 s_{24}^2) \right. \\
&\quad \left. + 2c_{14} s_{14} c_{23} s_{23} s_{13} s_{24} \cos \delta_3 \right] \sin^2 \left(\frac{\Delta m_{23}^2 L}{4E} \right).
\end{aligned} \tag{15}$$

Notice that the physical phase appears in $P_{CP}(\nu_e \rightarrow \nu_\tau)$ and $P_{CP}(\nu_\mu \rightarrow \nu_\tau)$ in a pure cosine dependence. Actually, no CP-odd observable can be built out of the oscillation probabilities in this approximation in spite of the existence of a physical CP-odd phase in the mixing matrix.

The existing experimental data impose some constraints on the parameter space, but still leave free a large range of angles and phases.

Bugey and Chooz are sensitive to the oscillation $\bar{\nu}_e \rightarrow \bar{\nu}_e$,

$$P(\bar{\nu}_e \rightarrow \bar{\nu}_e) = 1 - 4c_{23}^2 c_{24}^2 (s_{24}^2 + s_{23}^2 c_{24}^2) \sin^2 \left(\frac{\Delta m_{23}^2 L}{4E} \right). \tag{16}$$

The resulting bound is

$$(c_{23}^2 \sin^2 2\theta_{24} + c_{24}^4 \sin^2 2\theta_{23}) \leq 0.2 , \quad (17)$$

where Bugey gives a slightly stronger constraint in the larger mass range allowed by LSND. In our computations we safely stay within both experimental constraints. Notice that in the assumption of small angles, this bound forces the mixings s_{23}^2 and s_{24}^2 to be small and leaves more freedom in the mixings of the sterile neutrino: s_{13}^2 and s_{14}^2 .

On the other hand, the LSND signal of $\nu_e \rightarrow \nu_\mu$ transitions indicates a bound for the combination $10^{-3} \leq c_{13}^2 c_{24}^2 \sin^2 2\theta_{23} \leq 10^{-2}$, depending on the LSND mass difference. This bound fits nicely with the Chooz constrain to select a small s_{23}^2 .

We choose to be “conservative”, or even “pessimistic”, in order to illustrate the potential of the neutrino factory. In the numerical computations below we will make the assumption that all angles crossing the large LSND gap, θ_{13} , θ_{14} , θ_{23} and θ_{24} are small.

The large LSND mass difference, $\Delta m_{23}^2 \simeq 1\text{eV}^2$, calls for a SBL experiment rather than a LBL one. For illustration we consider in what follows an hypothetical 1 Ton detector located at $\simeq 1$ km distance from the neutrino source. We assume that the detector has τ tracking and μ and τ charge identification capabilities. We consider a muon beam of $E_\mu = 20$ GeV, resulting in $N_{CC} \simeq 10^7$ charged leptons detected, for a beam intensity of 2×10^{20} useful μ^- per year. An efficiency of $\epsilon_\mu = 0.5$, $\epsilon_\tau = 0.35$ for μ and τ detection respectively, and a background contamination at the level of $10^{-5} N_{CC}$ events are included.

• θ_{23} and θ_{13} from μ channels

The μ^+ appearance channel is particularly sensitive to θ_{23} . Fig. 4 shows the sensitivity reach in the $s_{23}^2/\Delta m_{23}^2$ plane for different values of θ_{13} . Inside the LSND allowed region the dependence on θ_{13} is mild: s_{23}^2 can reach 10^{-6} for $\theta_{13} \simeq 1^\circ$ or 6×10^{-6} for $\theta_{13} \simeq 60^\circ$.

Concerning the sensitivity to θ_{13} , Fig. 5 (left) illustrates the reach from μ appearance measurements in the $s_{13}^2/\Delta m_{23}^2$ plane, for different values of θ_{23} . Inside the LSND allowed region, the sensitivity to this angle strongly depends on the value of θ_{23} , with the larger sensitivity attained for large values of θ_{23} , a scenario somewhat disfavoured by the LSND measurement. For small values of θ_{23} ($\simeq 1^\circ$), the smallest testable value of s_{13}^2 is $\sim 10^{-2}$. Nevertheless, in this range the muon disappearance channel proves quite more sensitive: Fig. 5 (right) goes down to s_{13}^2 as small as 10^{-4} for $\theta_{23} \simeq 1^\circ$.

• θ_{14} and θ_{24} from τ channels

The τ^- appearance channel is quite sensitive to both s_{14}^2 and s_{24}^2 . Fig. 6 illustrates the sensitivity to s_{14}^2 as a function of θ_{13} : for about 1° , sensitivities of the order of 10^{-2}

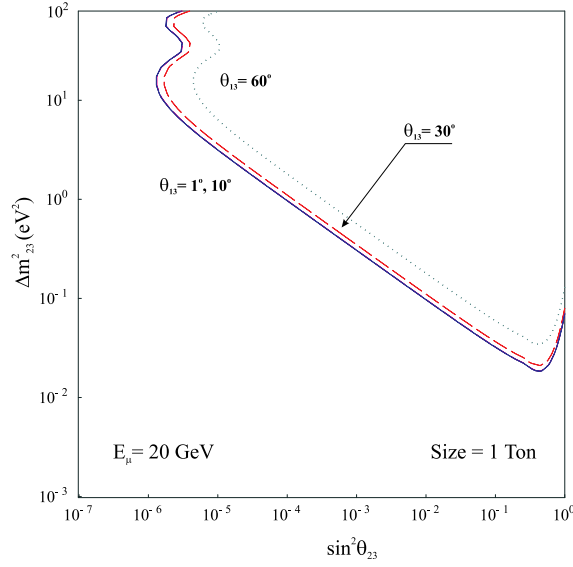


Figure 4: Sensitivity reach in the $s_{23}^2/\Delta m_{23}^2$ plane at different values of $\theta_{13} = 1^\circ, 10^\circ, 30^\circ$ and 60° for μ^+ appearance. We consider a 1 Ton detector at 1 km from the source and 2×10^{20} useful muons/year.

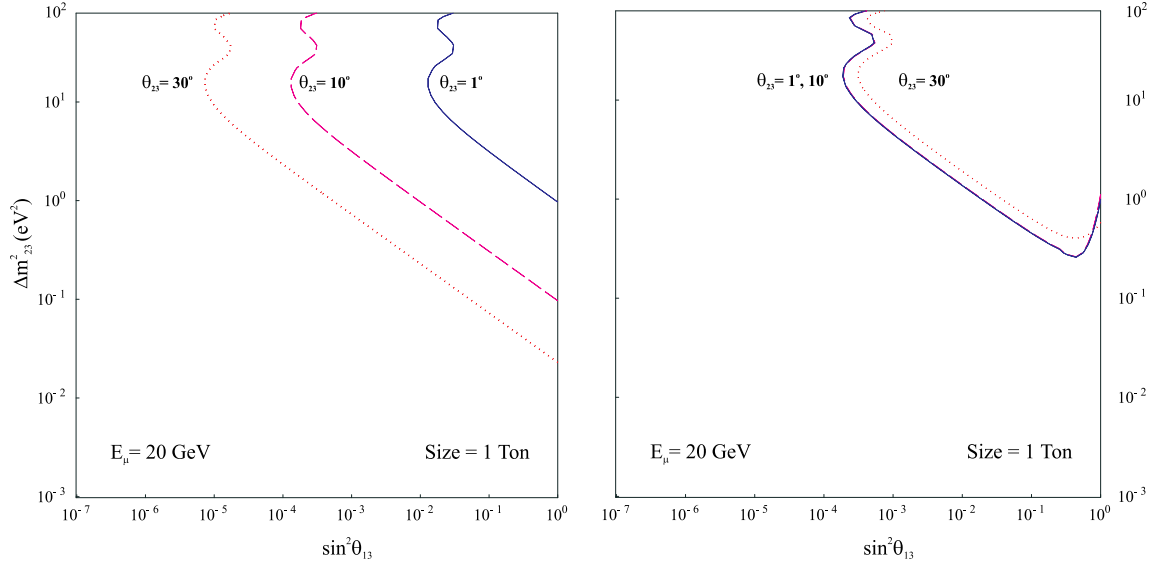


Figure 5: Sensitivity reach in the $s_{13}^2/\Delta m_{23}^2$ plane at different values of $\theta_{23} = 1^\circ, 10^\circ$ and 30° for μ^+ appearance (left) and disappearance (right). We consider a 1 Ton detector at 1 km from the source and 2×10^{20} useful muons/year.

are attainable, while for 10° the reach extends to 4×10^{-5} . For even larger values of θ_{13} it goes down to 10^{-6} (we recall that θ_{13} is not constrained by the present experimental bounds).

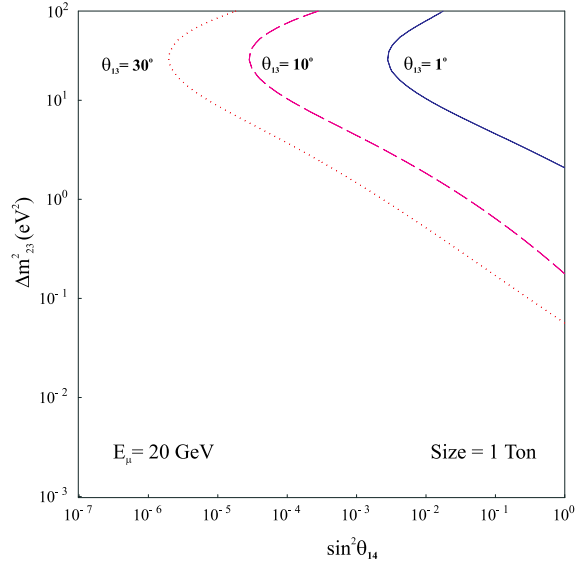


Figure 6: Sensitivity reach in the $s_{14}^2/\Delta m_{23}^2$ plane at different values of $\theta_{13} = 1^\circ, 10^\circ$ and 30° for τ^- appearance. We consider a 1 Ton detector at 1 km from the source and 2×10^{20} useful muons/year.

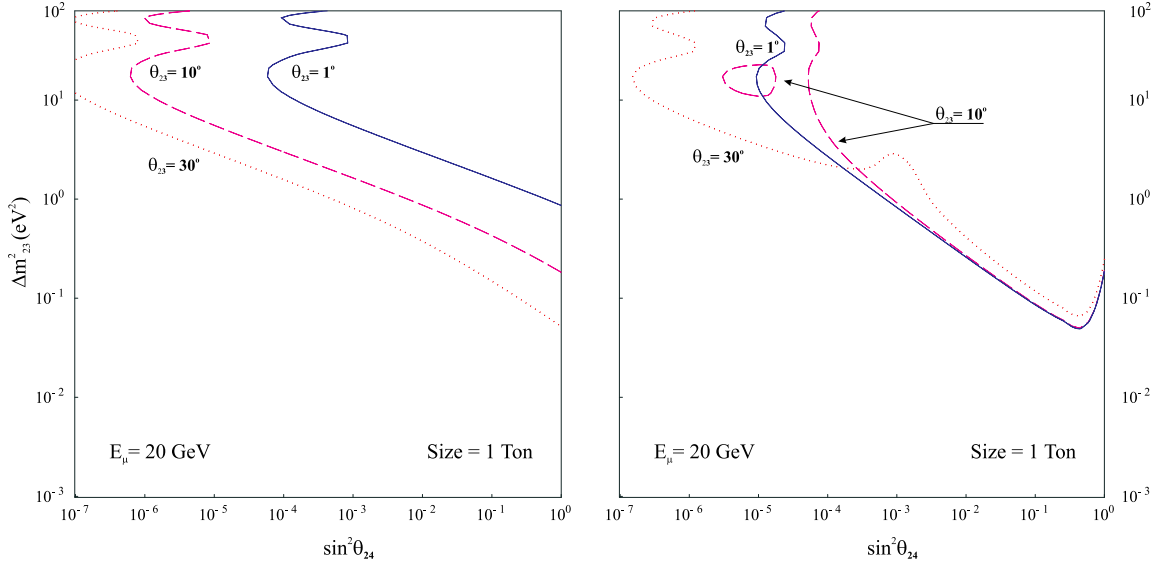


Figure 7: Sensitivity reach in the $s_{24}^2/\Delta m_{23}^2$ plane at different values of $\theta_{23} = 1^\circ, 10^\circ$ and 30° τ^+ appearance. We consider a 1 Ton detector at 1 km from the source and 2×10^{20} useful muons/year.

Fig. 7 (left) depicts the foreseeable sensitivity reach to s_{24}^2 as a function of θ_{23} : for small values of θ_{23} the sensitivity to s_{24}^2 goes down to 10^{-6} .

In contrast, the τ^+ appearance channel looks less promising. This is illustrated in

Fig. 7 (right): due to the relative negative sign between the two terms in the analytic expression for $P(\nu_e \rightarrow \nu_\tau)$, eq. (14), cancellations for particular values of the angles occur, resulting in a decreasing sensitivity in specific regions of the parameter space. For instance, for $\theta_{23} = 10^\circ$, the reach in s_{24}^2 splits into two separate regions for the LSND allowed range $\Delta m_{23}^2 \sim 10^1 \text{ eV}^2$. This sensitivity suppression is absent in the τ^- channel as the relative sign between the two terms in $P(\nu_\mu \rightarrow \nu_\tau)$, eq. (15), is positive.

The overall conclusion of this analysis is that, in the minimal scheme for four-neutrino families, a 1 Ton near detector with μ and τ charge identification is suitable to fully explore the CP-even part of the whole parameter space.

3.2 CP Violation with four light neutrino species

As in the standard three-family scenario, in order to reach observable CP-odd effects in oscillations it is necessary to have both physical CP-odd phases and at least two non-vanishing mass differences. The next-to minimal or “two mass scale dominance” scheme, described at the beginning of this section, is thus suitable.

As explained above, the parameter space consists of five angles and two CP-odd phases. Expanding the transition probabilities to leading order in Δm_{atm}^2 (i.e. Δm_{34}^2 in our parametrization), it follows that their CP-odd components are⁸:

$$P_{\mathcal{CP}}(\nu_e \rightarrow \nu_e) = P_{\mathcal{CP}}(\nu_\mu \rightarrow \nu_\mu) = P_{\mathcal{CP}}(\nu_\tau \rightarrow \nu_\tau) = 0, \quad (18)$$

$$P_{\mathcal{CP}}(\nu_e \rightarrow \nu_\mu) = 8c_{13}^2 c_{23}^2 c_{24} c_{34} s_{24} s_{34} \sin(\delta_2 + \delta_3) \left(\frac{\Delta m_{34}^2 L}{4E_\nu} \right) \sin^2 \left(\frac{\Delta m_{23}^2 L}{4E_\nu} \right), \quad (19)$$

$$\begin{aligned} P_{\mathcal{CP}}(\nu_e \rightarrow \nu_\tau) = & 4c_{23} c_{24} \left\{ 2c_{14} s_{14} c_{23} s_{23} s_{13} s_{24} (s_{13}^2 s_{14}^2 - c_{14}^2) \sin(\delta_2 + \delta_3) \right. \\ & + c_{14} c_{34} s_{13} s_{14} s_{34} \left[(s_{23}^2 - s_{24}^2) \sin \delta_2 + s_{23}^2 s_{24}^2 \sin(\delta_2 + 2\delta_3) \right] \\ & \left. + c_{14} c_{24} s_{13} s_{14} s_{23} s_{24} (c_{34}^2 - s_{34}^2) \sin \delta_3 \right\} \left(\frac{\Delta m_{34}^2 L}{4E_\nu} \right) \sin^2 \left(\frac{\Delta m_{23}^2 L}{4E_\nu} \right), \end{aligned} \quad (20)$$

$$\begin{aligned} P_{\mathcal{CP}}(\nu_\mu \rightarrow \nu_\tau) = & 8c_{13}^2 c_{23}^2 c_{24} c_{34} s_{34} \left[c_{14} c_{23} s_{13} s_{14} \sin \delta_2 + c_{14}^2 s_{23} s_{24} \sin(\delta_2 + \delta_3) \right] \times \\ & \left(\frac{\Delta m_{34}^2 L}{4E} \right) \sin^2 \left(\frac{\Delta m_{23}^2 L}{4E} \right). \end{aligned} \quad (21)$$

Two distinct phases appear, δ_2 and δ_3 , in a typical sinusoidal dependence which is the trademark of CP-violation and ensures different transition rates for neutrinos and antineutrinos.

CP-odd effects are observable in “appearance” channels, while “disappearance” ones are only sensitive to the CP-even part. The latter is mandated by CPT [20]. In contrast with the three-neutrino case, the solar suppression (see [7]) is now replaced

⁸At this order also sub-leading in the CP-even sector contribute. Although we do not illustrate them, all orders in Δm_{atm}^2 are included in the numerical computations.

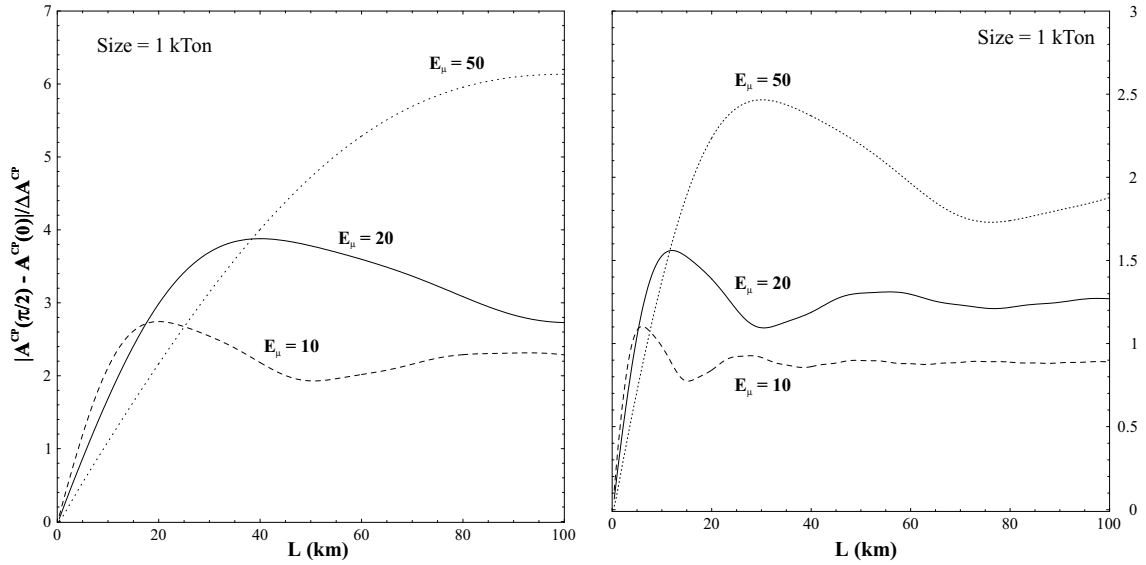


Figure 8: *Signal over statistical uncertainty for CP violation, in the $\nu_e \rightarrow \nu_\mu$ channel, for the two sets of parameters described in the text (Set 1 on the left and Set 2 on the right). We consider a 1 kTon detector and 2×10^{20} useful muons/year.*

by the a less severe atmospheric suppression. CP-violating effects are then expected to be one or two orders of magnitude larger than in the standard case, and independent of the solar parameters.

Staying in the “conservative” assumption of small $\theta_{13}, \theta_{14}, \theta_{23}, \theta_{24}$, we compare two democratic scenarios, in which all these angles are taken to be small and of the same order:

1. Set 1: $\theta_{34} = 45^\circ$, $\theta_{ij} = 5^\circ$ and $\Delta m_{atm}^2 = 2.8 \times 10^{-3} \text{ eV}^2$ for $\Delta m_{LSND}^2 = 0.3 \text{ eV}^2$;
2. Set 2: $\theta_{34} = 45^\circ$, $\theta_{ij} = 2^\circ$ and $\Delta m_{atm}^2 = 2.8 \times 10^{-3} \text{ eV}^2$ for $\Delta m_{LSND}^2 = 1 \text{ eV}^2$.

The value chosen for Δm_{atm}^2 is the central one of the most recent SuperK analysis [1]. In the figures below, the exact formulae for the probabilities have been used.

The size of the CP-asymmetries is very different for μ channels and τ channels. For instance for Set 2, they turn out to be small in $\nu_e - \nu_\mu$ oscillations, ranging from the permil level to a few percent. In contrast, in $\nu_\mu - \nu_\tau$ oscillations they attain much larger values of about 50% – 90%. This means that their hypothetical measurement should be rather insensitive to systematic effects, and other conventional neutrino beams from pion and kaon decay could be appropriate for their study.

• μ appearance channels

Fig. 8 shows the signal over noise ratio for the integrated CP asymmetry, eqs. (7), in the wrong sign muon channel, that is $\nu_e \rightarrow \nu_\mu$ versus $\bar{\nu}_e \rightarrow \bar{\nu}_\mu$ oscillations, as a function of

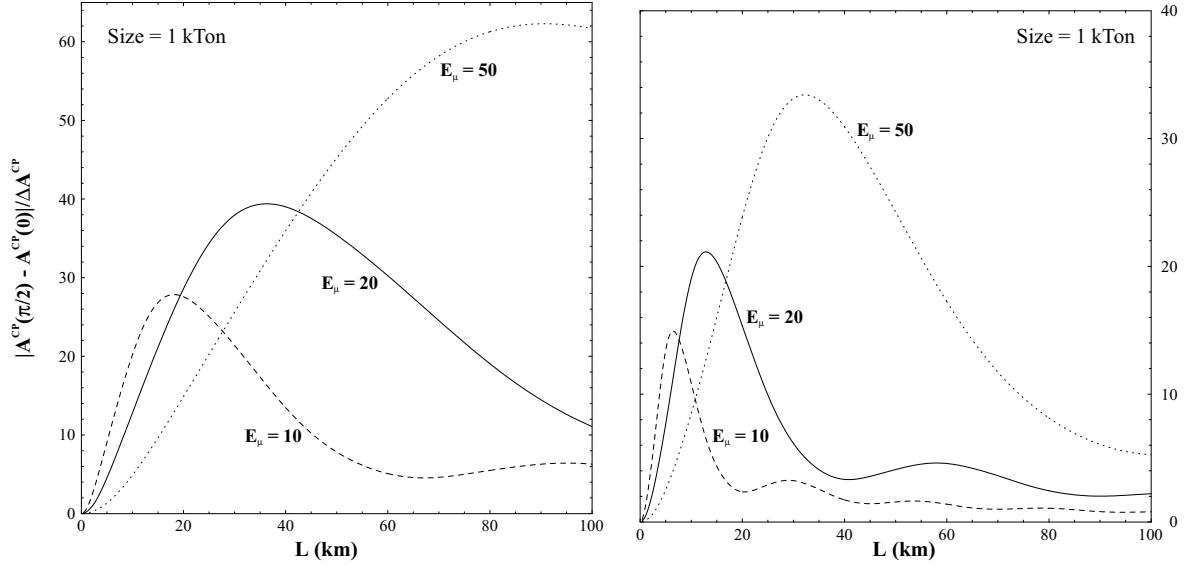


Figure 9: *Signal over statistical uncertainty for CP violation, in the $\nu_\mu \rightarrow \nu_\tau$ channel, for the two sets of parameters described in the text (Set 1 on the left and Set 2 on the right). We consider a 1 kTon detector and 2×10^{20} useful muons/year.*

the distance. Matter effects, although negligible, have been included. For the scenario and distances discussed here, the scaling laws are analogous to those derived for three neutrino species in vacuum, eq. (8), that is

$$\frac{A_{e\mu}^{CP}}{\Delta A_{e\mu}^{CP}} \propto \sqrt{E_\nu} \left| \sin \left(\frac{\Delta m_{34}^2 L}{4E_\nu} \right) \right|. \quad (22)$$

The maxima of the curves move towards larger distances when the energy of the muon beam is increased, or the assumed LSND mass difference is decreased. Moreover, increasing the energy enhances the significance of the effect at the maximum as expected. At $E_\mu = 50$ GeV, 6 standard deviation (sd) signals are attainable at around 100 km for the values in Set 1, and just 2.5 sd at 30 km for Set 2, levelling off at larger distances and finally diminishing when E_ν/L approaches the atmospheric range.

• τ appearance channels

In Fig. 9 we show the signal over noise ratio in $\nu_\mu \rightarrow \nu_\tau$ versus $\bar{\nu}_\mu \rightarrow \bar{\nu}_\tau$ oscillations as a function of the distance. The experimental asymmetry is obtained from eq. (7), with the obvious replacements $e \rightarrow \mu$ and $\mu \rightarrow \tau$. A larger enhancement takes place in this channel as compared to the $\nu_e \rightarrow \nu_\mu$ one. over 60 sd for Set 1 and 33 sd for Set 2 are a priori attainable. These larger factors follow from the fact that the CP-even transition probability $P_{CP}(\nu_\mu \nu_\tau)$ is smaller than $P_{CP}(\nu_e \nu_\mu)$, due to a stronger suppression in small mixing angles. Notice that the opposite happens in the 3-species case. Bilenky *et al.*

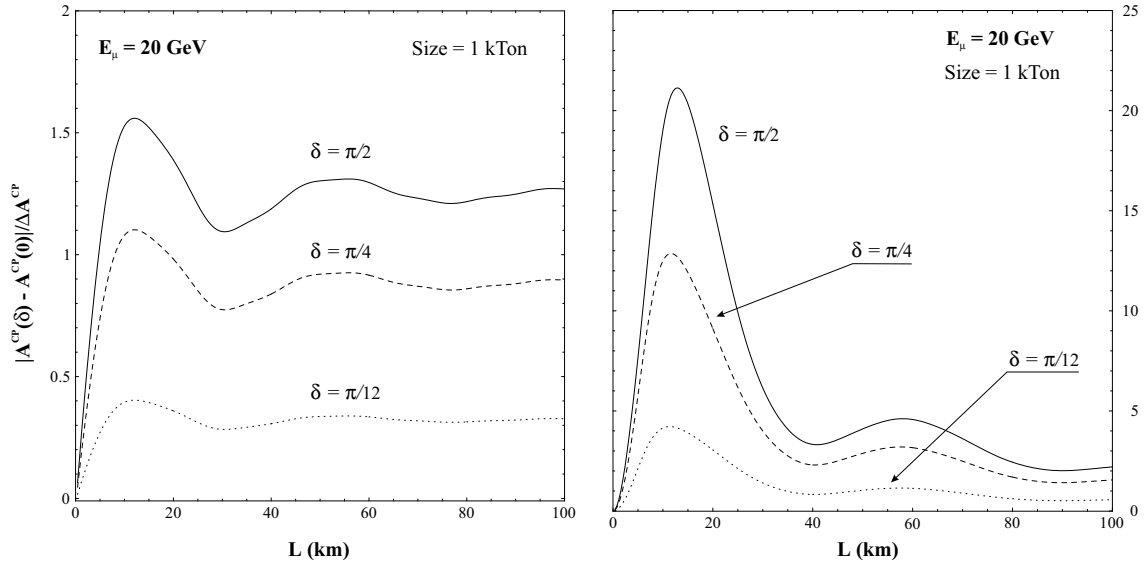


Figure 10: *CP violation asymmetry in the $\nu_e \rightarrow \nu_\mu$ (left) and $\nu_\mu \rightarrow \nu_\tau$ (right) channel for $E_\mu = 20$ GeV, angles and mass differences as in Set 2 and for different choice of the CP phases: $\delta_1 = \delta_2 = \delta_3 = \pi/2$ (full line), $\pi/4$ (dashed line) and $\pi/12$ (dotted line). We consider a 1 kTon detector from the source of a 2×10^{20} muon/year beam.*

[19] had previously concluded that the τ channel was best for CP-studies in the four species scenario. Their argument relied, though, on the fact that the parameter space involved in ν_τ oscillations is experimentally less constrained than the ν_μ one, a freedom we have not used here, staying within the more natural assumption that all the angles in the next-to-minimal scheme, except the atmospheric one, θ_{34} , are small.

The results in the $\nu_e \rightarrow \nu_\tau$ channels are almost identical to the $\nu_e \rightarrow \nu_\mu$ ones, not deserving a separate discussion.

The phase dependence is shown in Fig. 10, with the expected depletion of the signal for small CP phases. For small values of the phases, i.e. $\delta_1 = \delta_2 = \delta_3 = 15^\circ$, the significance drops to the 1σ level.

4 Summary.

The ensemble of solar plus atmospheric neutrino data, when analysed in a three-generation mixing scenario, points out the importance of long baseline experiments searching for $\nu_e \leftrightarrow \nu_\mu$ transitions. This is particularly relevant for determining θ_{13} and CP-odd effects. A neutrino factory from muon storage beams has much higher precision and discovery potential than any other planned facility. The number of useful observables is sufficient to determine or very significantly constrain the parameters θ_{23} and θ_{13} and Δm_{23}^2 of a standard three-generation mixing scheme. Experiments search-

ing for the appearance of “wrong sign” muons are very sensitive to the parameter space. For instance, while all other planned experiments will reach at most sensitivities of $\sin^2(\theta_{13}) > 10^{-2}$, much lower values are attainable at the neutrino factory, $\sin^2(\theta_{13}) > 10^{-4}$. For CP-violation we have updated previous studies, based in “ μ appearance” channels, which are the most promising ones, and derived the scaling laws with distance and energy of CP-odd observables. A fair chance to observe a significant signal of CP-violation requires that nature chooses Δm_{solar}^2 in the higher range allowed by the ensemble of solar experiments, $\Delta m_{solar}^2 \sim 10^{-4} \text{ eV}^2$ and that the solar mixing is large⁹. In other words, it requires that the large mixing angle solution (LMA-MSW) of the solar deficit is confirmed by the solar experiments. Would that be the case, a neutrino factory with high intensity muon beams ($\sim 10^{21}$ muons decaying in the direction of the detector) could be precise enough to discover CP-violation in the lepton sector. Matter effects in the energy integrated CP-odd observables that we have considered get more easily disentangled from the truly CP-violating effects the smaller θ_{13} is.

When the LSND signal is also taken into account, the reach of short base line experiments is extremely large. We have derived one and two mass scale dominance approximations, appropriate for CP-even and CP-odd observables, respectively. The plethora of channels for different flavours provided by the neutrino factory allows to cover the full mixing parameter space. CP violation may then be easily at reach, specially through “ τ appearance” signals. In these channels the CP-asymmetries are so large that even neutrino beams from conventional pion and kaon decays may be sufficient for their detection.

5 Acknowledgements

We acknowledge useful conversations with: B. Autin, R. Barbieri, J. Bernabeu, S. Bilenky, C. Giunti, A. De Rújula, F. Dydak, J. Ellis, J. Gómez-Cadenas, M.C. Gonzalez-Garcia, O. Mena, S. Petcov, C. Quigg and A. Romanino. A. D., M. B. G., and S. R. thank the CERN Theory Division for hospitality during the final stage of this work; their work was also partially supported as well by CICYT project AEN/97/1678. A. Donini acknowledges the I.N.F.N. for financial support. S. Rigolin acknowledges the European Union for financial support through contract ERBFMBICT972474.

References

- [1] Y. Fukuda *et al.*, Phys. Lett. **B433**(1998) 9, hep-ex/9805006, Phys. Rev. Lett. **81** (1998) 1562; T. Kagita, in Proceedings of the XVIIIth International Conference on

⁹If the results of some solar neutrino experiment are disregarded allowing for larger value for the solar mass difference, i.e. $\Delta m_{solar}^2 = 8 \cdot 10^{-4} \text{ eV}^2$, a promising signal follows even with moderate neutrino fluxes, as discussed in the text.

Neutrino Physics and Astrophysics, Takayama, Japan (June 1998).

- [2] L. Wolfenstein, Phys. Rev. **D17**(1978) 2369; **D20** (1979) 2634; S.P. Mikheyev and A. Yu Smirnov, Sov. J. Nucl. Phys. **42**(1986) 913.
- [3] B. Pontecorvo, Sov. Phys. JETP **26**, 984 (1968).
- [4] C. Athanossopoulos *et al.*, Phys. Rev. Lett. **81** (1998) 1774; Phys. Rev. C **58** (1998) 2489.
- [5] J. T. Peltoniemi and J. W. F. Valle, Nucl. Phys. B40693409; D. Caldwell and R. N. Mohapatra, Phys. Rev.D50943477; G. M. Fuller, J. R. Primack and Y.-Z. Qian, Phys. Rev.D52951288; J. J. Gomez-Cadenas and M. C. Gonzalez-Garcia, Zeit. Phys.C7196443; E. Ma and P. Roy, Phys. Rev.D5295R4780; E. Ma and J. Pantaleone, Phys. Rev.D5295R3763; R. Foot and R. R. Volkas, Phys. Rev.D52956595; Z. G. Berezhiani and R. N. Mohapatra, Phys. Rev.D52956607; E. J. Chun, A. S. Joshipura and A. Y. Smirnov, Phys. Lett.B35795608; Q. Y. Liu and A. Yu. Smirnov, hep-ph/9712493; V. Barger, K. Whisnant and T. Weiler, Phys. Lett. **B427**, 97 (1998) ; S. C. Gibbons, R. N. Mohapatra, S. Nandi and A. Raychaudhuri, Phys. Lett. **B430**, 296 (1998).
- [6] S. Geer, Phys. Rev **D57** (1989) 6989. B. Autin *et al.*, CERN-SPSC/98-30, SPSC/M 617 (October 1998).
- [7] A. de Rujula, M.B. Gavela and P. Hernandez, Nucl. Phys. **B547** (1999) 21.
- [8] Nufact '99 Workshop, July 5-9th, Lyon.
- [9] A. Cervera, F. Dydak and J. Gómez-Cadenas, Nufact '99 Workshop, July 5-9th, Lyon.
- [10] G.L. Fogli, E. Lisi, A. Marrone and G. Scioscia, hep-ph/9904465.
- [11] K. Dick, M. Freund, M. Lindner and A. Romanino, hep-ph/9903308.
- [12] V. Barger, S. Pakvasa, T. J. Weiler, K. Whisnant, hep-ph/9806328.
- [13] J. Arafune, M. Koike and J. Sato, Phys. Rev. **D 56** (1997) 3093, hep-ph/9703351. M. Tanimoto, Phys. Lett **B 345** (1998) 373, hep-ph/9806375. H. Minakata and H. Nunokawa, Phys. Lett. **B413** (1997) 369; Phys. Rev. **D57** (1998) 4403. M. Tanimoto, hep-ph/9906516.
- [14] N. Cabibbo, Phys. Lett. **B72** (1978) 33.
- [15] M. Apollonio *et al.*, Phys. Lett. **B338** (1998) 383.
- [16] A. Donini, M.B. Gavela, P. Hernández and S. Rigolin in proceedings of NuFact '99.

- [17] H.W. Zaglauer and K.H. Schwarzer, Z. Phys. **C 40** (1988) 273.
- [18] C. Caso *et al.*, EPJ **C3** (1998), 319.
- [19] S. M. Bilenky *et. al.*, hep-ph/9903454, hep-ph/9906251.
- [20] J. Bernab  u, hep-ph/9904474.
- [21] S. M. Bilenky, C. Giunti and W. Grimus, Phys. Rev. **D58** (1998) 033001. A recent four species analysis for long basexline experiments can be found in ref. [11].